Microkinetic Analysis of Ethanol to 1,3-Butadiene Reactions over MgO-SiO_2 Catalysts Based on Characterization of Experimental Fluctuations

Simoní Da Ros[a], Matthew D. Jones[b], Davide Mattia[c], Marcio Schwaab[d], Elisa Barbosa-Coutinho[e], Raimundo C. Rabelo-Neto[f], Fábio Bellot Noronha[f], José Carlos Pinto[a,*]

[a] Programa de Engenharia Química/COPPE, Universidade Federal do Rio de Janeiro, Cidade Universitária-CP: 68502, 21941-972, Rio de Janeiro, Brasil

[b] Department of Chemistry, University of Bath, Claverton Down, Bath BA2 7AY, UK

[c] Department of Chemical Engineering, University of Bath, Claverton Down, Bath BA2 7AY, UK

[d] Departamento de Engenharia Química, Universidade Federal do Rio Grande do Sul, Rua Engenheiro Luiz Englert, s/nº, 90040-040, Porto Alegre, Brasil

[e] Departamento de Físico-Química, Instituto de Química, Universidade Federal do Rio Grande do Sul, Av. Bento Gonçalves 9500, 91501-970, Porto Alegre, Brasil

[f] Catalysis Division, National Institute of Technology, Av. Venezuela 82, 20081312, Rio de Janeiro, Brazil

*Corresponding author, E-mail: pinto@peq.coppe.ufrj.br

Abstract

Microkinetic analysis of ethanol to 1,3-butadiene reactions over MgO-SiO_2 catalysts was performed based on the detailed characterization of experimental fluctuations, taking into account the influence of the reaction temperature and catalyst properties on ethanol conversion and product selectivities. The obtained results show that both reaction temperature and catalysts properties affected experimental fluctuations significantly. The local microkinetic information contained in the covariance matrix of experimental fluctuations indicated the change of the rate-limiting step as reaction temperature increased: from 300 to 400 ºC, the rate-limiting step was identified as the acetaldehyde condensation, while at 450 ºC, ethanol dehydrogenation step limits the 1,3-butadiene production.

Keywords: Ethanol; 1,3-butadiene; kinetics; rate-limiting step; experimental error; heterogeneous catalysis.

1. Introduction

The use of ethanol as a renewable source can be attractive for the production of different chemicals, such as ethene, propene, ethyl acetate, diethyl ether, acetaldehyde, ethylene oxide and 1,3-butadiene (1,3-BD) [1]. In particular, conversion of ethanol into 1,3-BD constitutes a promising green alternative for production of different polymer materials, including styrene-butadiene-rubber, polybutadiene, styrene-butadiene latex, acrylonitrile-butadiene-styrene rubber, and copolymers of butadiene and adiponitrile, acrylonitrile, chloroprene, styrene, among other monomers [2].

In order to produce 1,3-BD from ethanol, however, special catalysts are required, as the conversion of ethanol into 1,3-BD involves a complex network of consecutive reactions, which must be promoted by distinct active sites [3-10]. According to the usual reaction scheme, ethanol must first be dehydrogenated into acetaldehyde. Then, 3-hydroxybutanal must be formed through acetaldehyde self-aldolisation. Next, 3-hydroxybutanal must dehydrate into crotonaldehyde, which must then be reduced with ethanol to produce crotyl alcohol and acetaldehyde (Meerwein-Ponndorf-Verley (MPV) reduction). Finally, crotyl alcohol must be dehydrated to afford 1,3-BD. Taking into account this reaction route, the aldol condensation step has been assumed to be the most probable rate-limiting step over Ag/Zr/SiO_2 [7], Ag/MgO-SiO_2 [11], Zn/MgO-SiO_2 [12] and Al_2O_3-ZnO [13] catalysts, while ethanol dehydrogenation has been assumed to be the rate-limiting step over MgO-SiO_2 catalysts [3,11,12,14].

Based on the proposed reaction scheme, the ideal catalyst should contain both basic and acidic sites, distributed homogeneously throughout the catalyst surface [6]. However, ethanol dehydration into ethene and diethyl ether are also expected to constitute an unwanted competitive reaction, due to the presence of acidic sites on the catalyst surface [10]. Thus, considerable effort has been concentrated on the careful catalyst design [15] for proper

balancing of obtained reaction products, with much less attention dedicated to effects of operation variables (such as temperature, pressure and compositions) on the overall process performance for a particular catalyst.

In spite of that, the appropriate design, optimization and control of the overall reaction process require the adequate description of reaction phenomena with help of mathematical models, in order to represent the underlying relationships among independent (e.g. reaction temperature, feed concentration and residence time) and dependent variables (e.g. ethanol conversion and 1,3-BD selectivity). Besides, the kinetic mechanism can be better understood when more fundamental rate equations can be proposed, allowing for estimation of kinetic parameters and equilibrium constants [16].

During the model building process, model parameters must be estimated using the available experimental data. This process involves the minimization of an objective function that measures the distance between model predictions and observed experimental results. When experimental data follow the normal distribution and the independent variables are known with good precision, the objective function can usually be written in the form [17,18]:

$$S(\boldsymbol{\theta}) = (\mathbf{y}^{*} - \mathbf{y}^{e})^{T} \mathbf{V}^{-1} (\mathbf{y}^{*} - \mathbf{y}^{e}) \tag{1.1}$$

where $\mathbf{y}^{*}$ is the vector of model responses , $\mathbf{y}^{e}$ is the vector of experimental responses and $\mathbf{V}$ is the covariance matrix of experimental fluctuations. Since model responses must be described as functions of the independent variables, $\mathbf{x}^{*}$, and of the model parameters, $\boldsymbol{\theta}$, as

$$\mathbf{y}^{*} = f(\mathbf{x}^{*}, \boldsymbol{\theta}) \tag{1.2}$$

the minimization of Eq. (1.1) in fact requires the determination of the parameter values that lead to the point of minimum of the objective function defined by Eq. (1.1). However, as the

experimental data contain unavoidable experimental uncertainties, parameter estimates are also uncertain to some extent. The parametric uncertainties are usually calculated with help of the covariance matrix of the parameter estimates, $\mathbf{V}_\theta$, defined as

$$\mathbf{V}_\theta = [\mathbf{B}^T \mathbf{V}_y^{-1} \mathbf{B}]^{-1} \tag{1.3}$$

where **B** is the sensitivity matrix that contains the first derivatives of the model responses in respect to the model parameters [17,18]. As the model parameters are uncertain, model predictions are also subject to uncertainties, which can be calculated in the form [19,20]:

$$\mathbf{V}_y = \mathbf{B}\mathbf{V}_\theta \mathbf{B}^T \tag{1.4}$$

As a consequence, the precise determination of experimental fluctuations is of fundamental importance for model building and evaluation of model adequacy, although careful determination of experimental errors is frequently overlooked in most kinetic studies.

It is also important to emphasize that available experimental data can often be explained by different mechanistic interpretations, particularly during the initial steps of investigations performed in the field of catalysis [16,21]. In this case, experimental design techniques can be employed for discrimination among rival models [20,22]. The main idea behind these techniques is to perform experiments at conditions that can lead to the maximum difference among the responses of the rival models, making model discrimination easier. In order to do that, different design criteria have been proposed in the literature [20,22,23]. For instance, Schwaab *et al*. [22] proposed the use of a discriminating function between rival models *m* and *n* that takes into account the probabilities P_m and P_n for the analyzed models to be the correct ones, in the form:

$$D_{m,n}(\mathbf{x}) = (P_m P_n)^z [\hat{\mathbf{y}}_m(\mathbf{x}) - \hat{\mathbf{y}}_n(\mathbf{x})]^T \mathbf{V}_{m,n}^{-1} \times [\hat{\mathbf{y}}_m(\mathbf{x}) - \hat{\mathbf{y}}_n(\mathbf{x})] \quad (1.5)$$

where z is a parameter used to modulate the relative importance of the rival models, $\hat{\mathbf{y}}_m$ is a vector of response variables for model m and $\mathbf{V}_{m,n}$ is defined as

$$\mathbf{V}_{m,n} = 2\mathbf{V}(\mathbf{x}) + \mathbf{V}_m(\mathbf{x}) + \mathbf{V}_n(\mathbf{x}) \quad (1.6)$$

where $\mathbf{V}$ is the covariance matrix of experimental fluctuations, as defined in Eq. (1.1), and $\mathbf{V}_m$ is the covariance matrix of model responses calculated for model m with Eq. (1.4). In order to find the maximum value of Eq. (1.5) (and the best set of experimental conditions for model discrimination), independent variables $\mathbf{x}$ must be manipulated with help of a numerical procedure. Once more, the detailed characterization of experimental fluctuations, contained in the covariance matrix $\mathbf{V}$, is of paramount importance during the model building process.

Usually, experimental fluctuations are assumed to be independent from each other and constant throughout the experimental region. These hypotheses allow for significant simplification of the objective function defined in Eq. (1.1), as the matrix $\mathbf{V}$ becomes diagonal and independent of the experimental conditions. However, it has been demonstrated that the use of such assumptions with no previous experimental evidence may lead to inconsistent kinetic conclusions [19]. Additionally, the proper characterization of the covariance matrix is fundamental in the computation of accurate kinetic parameters [19, 24].

It is also important to observe that characterization of V can also allow for detailed observation of local kinetic phenomena, defined here as microkinetic analysis [19]. The idea is simple and appealing: if the experimental fluctuations are not independent and are not constant (which can only be assured if detailed characterization of error fluctuations is performed), then the fluctuations of the distinct analyzed variables affect one another, revealing the underlying local reaction mechanism. The use of the words *"local"* and

"microkinetic" can be justified by the low magnitude of the error fluctuations when replicates are performed. For instance, these error fluctuations can be present due to small deviation in the mass catalyst used in replicates and, since catalyst mass affect all reactions simultaneously, the deviations in the replicates are connected with the particular reaction mechanism that is occurring on the catalyst surface. As a consequence, the covariance matrix of error fluctuations contains simultaneously information about the experimental errors and about the underlying kinetic mechanism, which can be used for model building and kinetic interpretation [19].

Based on the previous paragraphs, the main objective of the present manuscript is to analyze the production of 1,3-BD from ethanol, based on the detailed characterization of experimental fluctuations of various product concentrations in the output stream. Two MgO-SiO_2 catalyst systems (with Mg:Si molar ratios of 50:50 and 95:5) were studied, since these catalysts are employed widely for converting ethanol into 1,3-BD due to their characteristic multifunctional properties [6,10,25]. Particularly, the effects of the reaction temperature and catalyst properties on the covariance matrix of experimental fluctuations were investigated. It was observed that the covariance matrix of experimental fluctuations contained useful information about the reaction mechanism, suggesting the change of the rate-determining step when the reaction temperature was increased.

2. Materials and Methods

2.1 Catalyst Preparation

Catalysts with Mg:Si molar ratios of 50:50 and 95:5 were prepared by co-precipitation. For the 50:50 material, 9.01 g of SiO_2 (Sigma-Aldrich (SA), 99.8 %) was dissolved in 100 mL of 1.2 M NaOH solution (SA, 99 %). The mixture was heated between 60 and 80 °C under vigorous stirring until complete SiO_2 dissolution. The solution was cooled

and 42.4 g of Na_2CO_3 (SA, 99.9 %) were added. A $Mg(NO_3)_2 \cdot 6H_2O$ solution (SA, 99 %) was added drop-wise into this mixture whilst stirring at 25 °C (38.85 g of $Mg(NO_3)_2 \cdot 6H_2O$ in 200 mL). The pH was maintained at 10.5 by adding appropriate quantities of 1.2 M NaOH solution and, at the end of the process, the solution volume was adjusted to 600 mL with deionized water. The resulting mixture was stirred for 2 h before ageing for 22 h at 25 °C. Finally, the mixture was filtrated and washed with 7.5 L of hot water. The precipitate was dried at 80 °C for 24 h before grinding. Materials were calcined in air at 500 °C for 4 h, using a heating rate of 5 °C/min. Samples were labeled as MgO-SiO_2-*x*, where *x* represents the Mg:Si molar ratio.

2.2 Catalyst Characterization

Samples were characterized by nitrogen physisorption, powder X-ray diffraction and ^{29}Si solid-state nuclear magnetic resonance (NMR) spectroscopy as described elsewhere [10]. Basicity of catalyst samples was assessed by temperature programmed desorption of CO_2 (CO_2-TPD). A flow system coupled with an *in-line* mass spectrometer, Prisma™ Pfeiffer Vacuum Quadrupole, was used to measure the outgas composition. The release of CO_2 (m/z=44) was monitored. Prior to adsorption, the sample (200 mg) was pre-treated with helium flow for 1 h at 500 ºC (10 ºC/min). Samples were then exposed to CO_2 flow for 0.5 h at 100 ºC. The CO_2 excess was removed with helium flow at 100 °C for 1.5 h. The CO_2-TPD analyses were performed by heating the sample at rate of 10 °C/min from 100 to 700 °C and maintaining the temperature of 700 °C for 0.5 h, under helium.

X-ray fluorescence (XRF) was used in order to quantify the chemical composition of samples. Powdered samples (300 mg) were pressed at 27 kN/cm² to provide disks with diameters of 18 mm. The disks were then analyzed by XRF under vacuum, using a RIX 3100 RIGAKU spectrometer.

2.3 Catalytic Reactions

Catalytic reactions were performed in a flow quartz packed-bed reactor at atmospheric pressure. Nitrogen was used as diluent (15 ml/min). Before experiments, the catalyst sample (100 mg) was pre-treated with nitrogen flow for 1 h at 500 ºC (5 ºC/min). Reactions were then performed between 300 and 450 ºC, using an ethanol WHSV of 0.8 h^{-1}. Reaction products were analyzed after 0.5 h of time on stream (TOS) with help of a Micro GC Agilent 3000 instrument, equipped with three channels, three thermal conductivity detectors and three columns: a molecular sieve, a Poraplot Q and an OV-1 column. Ethanol conversion was calculated with Eq. (2.1), where $F_{EtOH,in}$ is the ethanol molar stream in the reactor inlet and $F_{EtOH,out}$ is the same stream in the reactor outlet.

$$X(\%) = \frac{(F_{EtOH,in} - F_{EtOH,out}) \cdot 100}{F_{EtOH,in}} \qquad (2.1)$$

Thermogravimetric analysis of used catalysts indicated no significant catalyst deactivation, as shown in Figure S1 in the Supporting Information (SI). Moreover, blank tests performed without the catalyst resulted in ethanol conversion approximately equal to zero (< 2 %, even at 450 ºC), suggesting that homogeneous gas phase reactions along the output lines were not important.

2.4 Characterization of Experimental Fluctuations

It must be noted that the term "experimental fluctuation" is used here to represent the total intrinsic experimental variability associated with composition measurements of unconverted ethanol and reaction products in the reactor outlet stream. Therefore, experimental fluctuations comprise the intrinsic fluctuations of both the analytic

chromatographic system and the reaction process, which are related to the composition measurements (see illustrative Scheme S1 in the Supplementary Information).

The intrinsic experimental fluctuations related to the analytic chromatographic system are referred here as the chromatographic measurement fluctuations (or only measurement fluctuations), while the intrinsic experimental fluctuations related to the catalytic experiments are referred here as the catalytic reaction fluctuations. However, catalytic reaction fluctuations cannot be determined independently from measurement fluctuations, since measurements obtained from process outputs present variability components originated from both catalytic and chromatographic systems and are, therefore, measures of the total experimental fluctuations. Thus, in order to discriminate measurement fluctuations from catalytic reaction fluctuations, both fluctuations were determined. Chromatographic measurement fluctuations were calculated through replication of chromatographic analysis at different composition conditions. In these replicate runs, chemical compounds were fed into the measuring system with help of a saturator (for ethanol and diethyl ether analyses) or from gas cylinders (for 1,3-butadiene, acetaldehyde, ethene, butene and hydrogen analyses). At least three replicates were performed for each composition condition. These experiments were used simultaneously to calibrate the GC instrument and to estimate measurement fluctuations. From these composition measurements, variances were calculated for each composition condition using Eq. (2.2), where s_{ij}^2 is the variance of observed molar fractions of compound *i* at condition *j*, y_{ij}^k is the *k*-th observation of the molar fraction of compound *i* at composition condition *j*, $\bar{y}_{ij}$ is the average of observed molar fractions of compound *i* at composition condition *j* and *NR* is the total number of replicates.

$$s_{ij}^2 = \frac{\sum_{k=1}^{NR} (y_{ij}^k - \bar{y}_{ij})^2}{NR - 1} \tag{2.2}$$

For characterization of catalytic reaction fluctuations, three experiments were performed at each reaction condition. The covariance matrix of catalytic reaction fluctuations

of composition measurements at each reaction condition was computed with Eq. (2.2) and Eq. (2.3), where s_{ij}^2 is the variance of observed molar fractions of compound *i* at reaction condition *j*, ξ_{il}^j denotes the covariance of observed molar fractions of compounds *i* and *l* at reaction condition *j*, y_{ij}^k is the *k*-th observation of the molar fraction of compound *i* at reaction condition *j*, $\bar{y}_{ij}$ is the average of observed molar fractions of compound *i* at reaction condition *j* and *NR* is the total number of replicates.

$$\xi_{il}^j = \frac{\sum_{k=1}^{NR}(y_{ij}^k - \bar{y}_{ij})(y_{lj}^k - \bar{y}_{lj})}{NR-1} \tag{2.3}$$

Finally, the correlation matrix of observed compositions at each reaction condition was calculated with Eq. (2.4), where ρ_{il}^j represents the correlation coefficient of observed molar fractions for compounds *i* and *l* at reaction condition *j*. Scheme S2 was included in the Supplementary Information to illustrate the processes used for calculation of covariance and correlation matrixes.

$$\rho_{il}^j = \frac{\xi_{il}^j}{s_{ij} \cdot s_{lj}} \tag{2.4}$$

3. Results and Discussion

3.1 Catalyst Properties

The effects of the Mg:Si molar ratio of MgO-SiO_2 catalysts prepared by co-precipitation on the performances of ethanol to 1,3-BD reactions have been studied previously [10]. The two catalyst samples investigated in the present work presented distinct crystalline structures. While diffraction patterns indicated amorphous features for the MgO-SiO_2-(50:50) sample, with broad peaks (at 25-30°, 33-39° and 58-62°) characteristic of magnesium silicate hydrates, the MgO-SiO_2-(95:5) sample presented diffractions at Bragg angles of 37º, 43º and

62º, suggesting the MgO periclase phase presence, Figure S2 [10,11]. Surface areas were equal to 368 and 135 m^2/g, as determined for the MgO-SiO_2-(50:50) and MgO-SiO_2-(95:5) samples, respectively [10]. To avoid internal pore diffusion limitations, catalysts particles were always grinded until sizes smaller than 53 μm. Furthermore, while a single nuclear magnetic resonance placed at -71 ppm in the ^{29}Si NMR spectra was observed for the MgO-SiO_2-(95:5) catalyst, indicating a high concentration of Q^1 species, resonances were shifted for the MgO-SiO_2-(50:50) sample to -87 and -94 ppm, suggesting an increase in Q^2 and Q^3 species, Figure S3 [10,11,26,27].

The chemical composition estimated by XRF presented satisfactory agreement between nominal and measured Mg:Si molar ratios, as described in Table S1 in the SI. Finally, CO_2-TPD experiments were used to assess the basicity of catalyst samples. A huge difference in the *m/z* signal attributed to CO_2 was observed, as shown in Figure S4 in the SI, indicating a higher concentration of basic sites for the MgO-SiO_2-(95:5) system, as expected.

3.2 Catalytic Reactions

The two catalysts, MgO-SiO_2-(50:50) and MgO-SiO_2-(95:5), were used to perform the ethanol reactions at different reaction temperatures. The main observed carbon containing products were ethene, 1,3-BD, acetaldehyde (AcH) and diethyl ether (DEE). In addition, traces of ethane, 1-butene, 2-butene, propene and CO_2 were also detected. Molar fractions of unconverted ethanol, main carbon containing products and hydrogen in the output stream are presented in Tables 1-2.

It must be noted that the main objective of the present manuscript is the characterization of the kinetic information contained in the covariance matrix of experimental catalytic reaction fluctuations. Thus, molar fractions were selected as representative output variables because they can be quantified directly through GC analyses, allowing for simpler discrimination between chromatographic measurement and catalytic reaction fluctuations.

Taking this into account, this section aims to present the experimental data used for characterization of catalytic reaction fluctuations. Table S2 of the Supplementary Information presents the catalyst performances in terms of yields at distinct reaction temperatures, including carbon balances, which were typically better than 85 % for reactions performed with the MgO-SiO_2-(50:50) system. Average selectivities obtained over the MgO-SiO_2-(50:50) catalyst are shown in Table S3 of the Supplementary Information.

Table 1 Output molar fractions stream of unconverted ethanol, main carbon containing products and hydrogen obtained with the MgO-SiO_2-(50:50) system (TOS = 0.5 h, WHSV = 0.8 h^{-1}, ethanol molar fraction equal to 0.06).

Reaction Temperature (ºC)	Molar fractions (%) [a]					
	Ethanol	1,3-BD	AcH	H_2	Ethene	DEE
300						
	5.621	0.048	0.070	0.031	0.063	0.080
	5.977	0.006	0.014	0.012	0.056	0.073
	5.836	0.009	0.018	0.029	0.053	0.072
350						
	4.813	0.061	0.053	0.086	0.617	0.219
	5.075	0.048	0.040	0.066	0.529	0.199
	4.949	0.043	0.041	0.084	0.499	0.202
400						
	1.941	0.193	0.087	0.249	2.785	0.160
	2.629	0.175	0.077	0.209	2.434	0.151
	2.412	0.178	0.085	0.241	2.418	0.195
450						

0.139	0.289	0.093	0.376	4.403	0.008
0.655	0.264	0.105	0.338	4.137	0.017
0.250	0.295	0.096	0.374	4.354	0.015

[a] Molar fractions do not present their sum next to 100 due to nitrogen (inert gas) and water molar fractions, which were omitted.

Table 2 Output stream molar fractions of unconverted ethanol, main carbon containing products and hydrogen obtained with the MgO-SiO_2-(95:5) system (TOS = 0.5 h, WHSV = 0.8 h^{-1}, ethanol molar fraction equal to 0.06).

Reaction Temperature (ºC)	Molar fractions (%)[a]					
	Ethanol	1,3-BD	AcH	H_2	Ethene	DEE
300						
	5.271	0.012	0.031	0.063	0.015	0.003
	5.308	0.012	0.034	0.059	0.014	0.003
	5.309	0.010	0.028	0.060	0.016	0.004
350						
	4.617	0.084	0.088	0.254	0.077	0.006
	4.702	0.071	0.087	0.225	0.081	0.008
	4.681	0.074	0.087	0.237	0.076	0.006
400						
	3.126	0.319	0.208	0.810	0.262	0.008
	3.220	0.291	0.193	0.733	0.283	0.011
	3.101	0.299	0.197	0.765	0.257	0.009
450						
	0.838	0.601	0.238	2.146	0.645	0.002
	0.961	0.583	0.237	2.006	0.689	0.009

	0.909	0.591	0.237	2.018	0.632	0.008

[a] Molar fractions do not present their sum next to 100 due to nitrogen (inert gas) and water molar fractions, which were omitted.

The average values of molar fractions of the main products in the output stream are plotted as functions of the reaction temperature in Figure 1 for catalysts MgO-SiO_2-(50:50) and MgO-SiO_2-(95:5). The vertical bars represent the absolute standard deviations, which were calculated with the replicates. It is important to observe that the existence of mass transfer limitation effects in the catalytic experiments could be neglected, as shown in Figure S5 of the Supplementary Information, after estimation of the apparent activation energies [10].

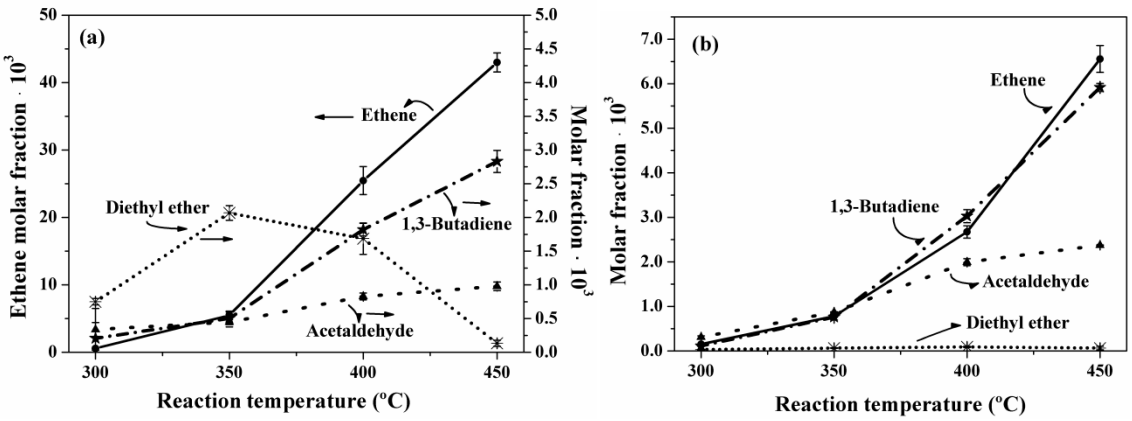

Figure 1 – Distribution of main carbon containing products: Ethene (●), 1,3-butadiene (★), diethyl ether (✳) and acetaldehyde (▲), for catalyst MgO-SiO_2-(50:50) (a) and MgO-SiO_2-(95:5) (b) as functions of reaction temperature (TOS = 0.5 h, feed rate of 0.8 g_{EtOH} g_{cat}^{-1} h^{-1}). Lines were drawn for clarity.

For catalyst MgO-SiO_2-(50:50), ethene was the main observed product from 350 to 400 ºC, while diethyl ether was the main product at 300 ºC. Average ethanol conversion ranged from 4.7 %, at 300 ºC, to 93.8 %, at 450 ºC, with standard deviation equal to 1.7 %

and 4.8 %, respectively. For catalyst MgO-SiO_2-(95:5), a different product distribution was obtained. In this case, the amounts of produced ethene were significantly smaller, when compared to the previous catalyst, although the amounts of 1,3-BD were similar. These results were in agreement with the higher basicity observed through CO_2-TPD characterizations for the MgO-SiO_2-(95:5) catalyst. The average ethanol conversion ranged from 6.2 %, at 300 ºC, to 83.0, at 450 ºC, with standard deviation equal to 3.4 % and 1.3 %. As expected, higher 1,3-BD, AcH and ethene molar fractions were observed with the increasing reaction temperature for both catalysts.

3.3 Characterization of Chromatographic Measurement Fluctuations

Measurement fluctuations (experimental fluctuations from chromatographic analysis) were first determined to differentiate them from catalytic reaction fluctuations. In order to do this, compounds were analyzed chromatographically using distinct molar fraction compositions (detailed in Table S4 in the SI), using at least three replicates. It must be emphasized that these tests were not performed under reaction conditions and that the compounds were fed directly into the gas chromatograph equipment.

Figure 2 shows the effect of the average molar fraction on the respective variance of molar fraction measurements for ethanol (a), 1,3-BD (b), AcH (c), hydrogen (d), ethene (e) and DEE (f). The increase of variance could be observed as the average molar fraction increased, resulting in the relative molar fraction variance (variance divided by the square of the molar fraction) being approximately constant. This clearly shows that the assumption of constant measurement fluctuations can be indeed a very poor assumption for quantitative data analysis. An empirical equation was then developed to describe molar fraction variance as a function of the average molar fraction. Data was well fitted by a quadratic function as $y = a \cdot x^2$, shown in Figure 2 as a line, where y represents the variance, x denotes the average molar fraction, and a is an empirical parameter, which is different for each compound and has the

same definition of the relative molar fraction variance. Figure S6 (in the SI) illustrates experimental relative molar fraction variances and the estimated empirical parameter *a* for each compound.

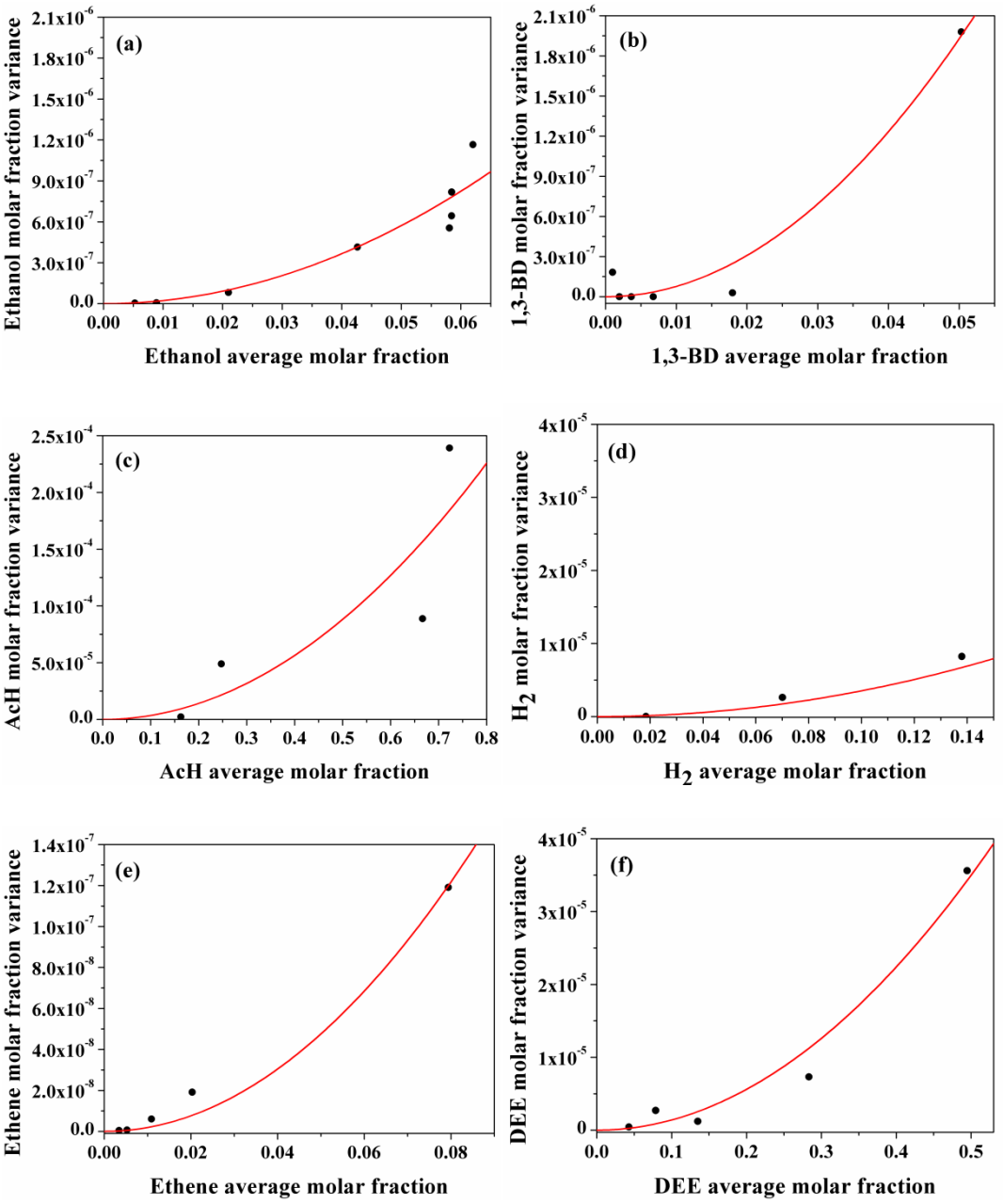

Figure 2 - Variance of molar fraction as function of average molar fraction from chromatographic analysis for ethanol (a), 1,3-BD (b), AcH (c), H_2 (d), ethene (e) and DEE (f): (●) experimental values, (-) empirical model.

The effect of average molar fraction on its variance can possibly be associated with modification of the equilibrium states during the chromatographic separation, as the molar fraction increases, due to column overloading and different retention strengths for each solute [28]. Change of the equilibrium states can result in wider chromatogram bandshapes, leading to an increase of the chromatographic variance [28].

3.4 Characterization of Catalytic Reactions Fluctuations

Variances of molar fractions measures in the output stream were calculated with data presented in Tables 1-2 and using Eq. (2.2) at each reaction temperature. The obtained variances were statistically different at each distinct reaction temperature and for the different catalysts, as verified with the standard F-test [29]. Consequently, the commonly used hypothesis of constant experimental error throughout whole experimental region should not be applied for this reaction system (and probably for many other ones, despite the widespread use of the constant variance assumption).

Since the different reaction temperatures and catalysts lead to different ethanol conversions and products compositions, one might wonder whether molar fraction variances were different because of the molar fraction effect on chromatographic measurement fluctuations (as explained in Section 3.3) or because of the distinct catalytic reaction fluctuations. However, with help of the standard F-test [29], it can be concluded that catalytic reaction fluctuations cannot be explained only by the chromatographic measurement fluctuations, as illustrated in Figures 3 to 8. As a consequence, it can be also concluded that there is at least one additional source of fluctuations in the reaction runs, other than the chromatographic measurement ones, and that this is related to the reaction phenomena itself (such as unavoidable fluctuation of catalyst activities, as discussed elsewhere [19,24]).

Figures 3-8 show variances of molar fraction measures obtained during catalytic reactions as functions of the average molar fraction for each compound. Each point is related to

one reaction temperature for catalysts MgO-SiO_2-(50:50) (a) and MgO-SiO_2-(95:5) (b). In these figures, the empirical equations obtained to explain the chromatographic measurement fluctuations were plotted as continuous lines in order to allow for better visualization of the differences observed between variances from measurement and from catalytic reactions fluctuations. It must be emphasized that all molar fractions obtained during reaction experiments were in the same experimental range used to characterize the chromatographic measurement fluctuations and to build the respective empirical models, so that the empirical models provide good references of chromatographic measurement fluctuations in the analyzed ranges of molar fractions obtained during the reaction runs.

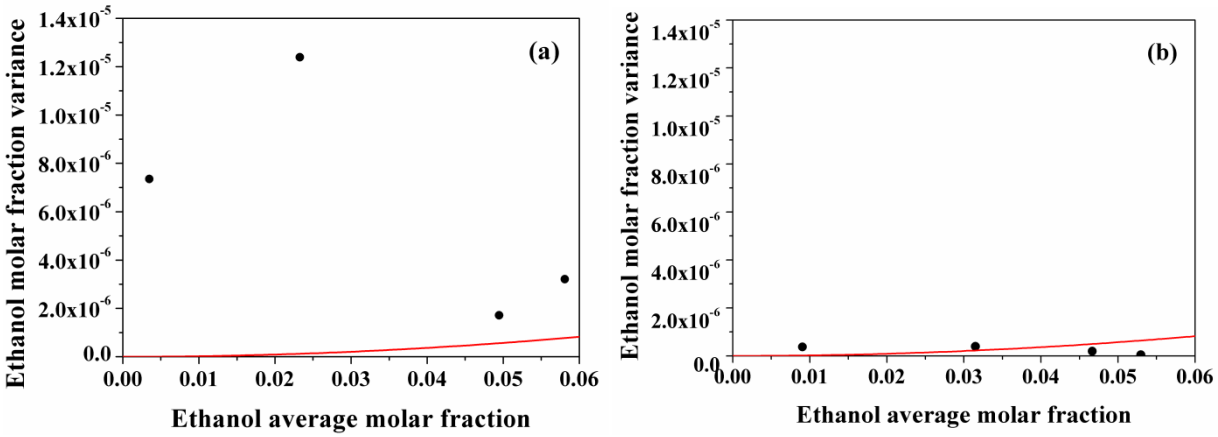

Figure 3 – Variances of ethanol molar fractions for catalytic reactions (●) and chromatographic measurement fluctuation model (-) as functions of ethanol average molar fractions for catalysts MgO-SiO_2-(50:50) (a) and MgO-SiO_2-(95:5) (b).

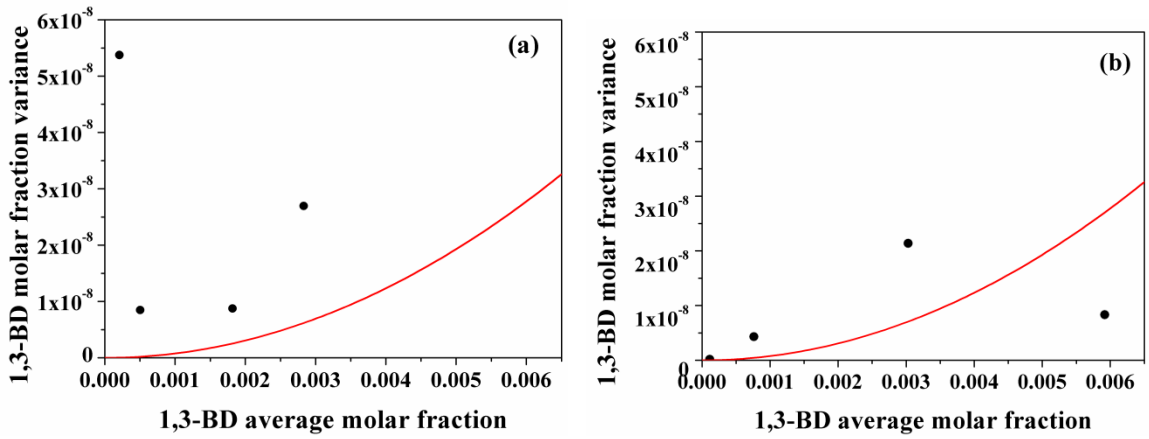

Figure 4 – Variances of 1,3-BD molar fractions for catalytic reactions (●) and chromatographic measurement fluctuation model (-) as functions of 1,3-BD average molar fractions for catalysts MgO-SiO_2-(50:50) (a) and MgO-SiO_2-(95:5) (b).

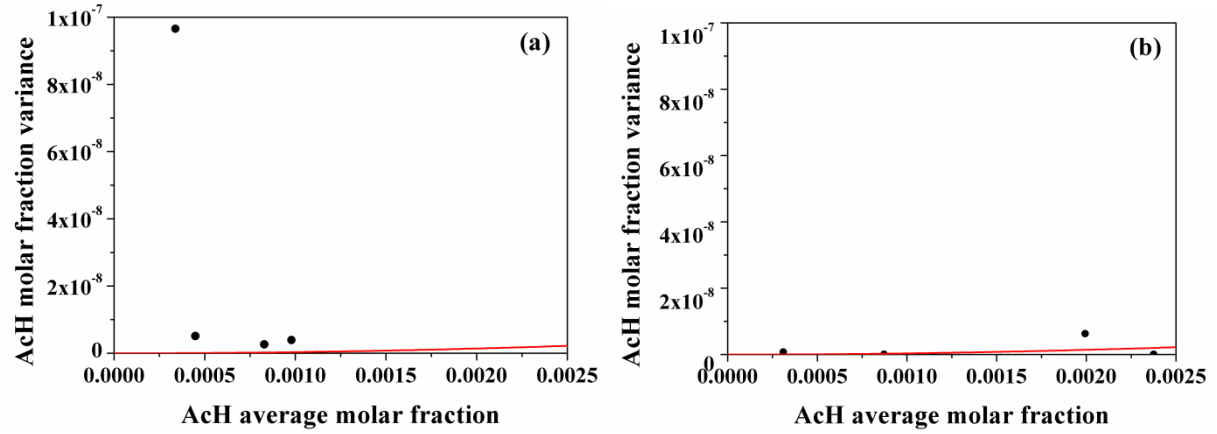

Figure 5 – Variances of AcH molar fractions for catalytic reactions (●) and chromatographic measurement fluctuation model (-) as functions of AcH average molar fractions for catalysts MgO-SiO_2-(50:50) (a) and MgO-SiO_2-(95:5) (b).

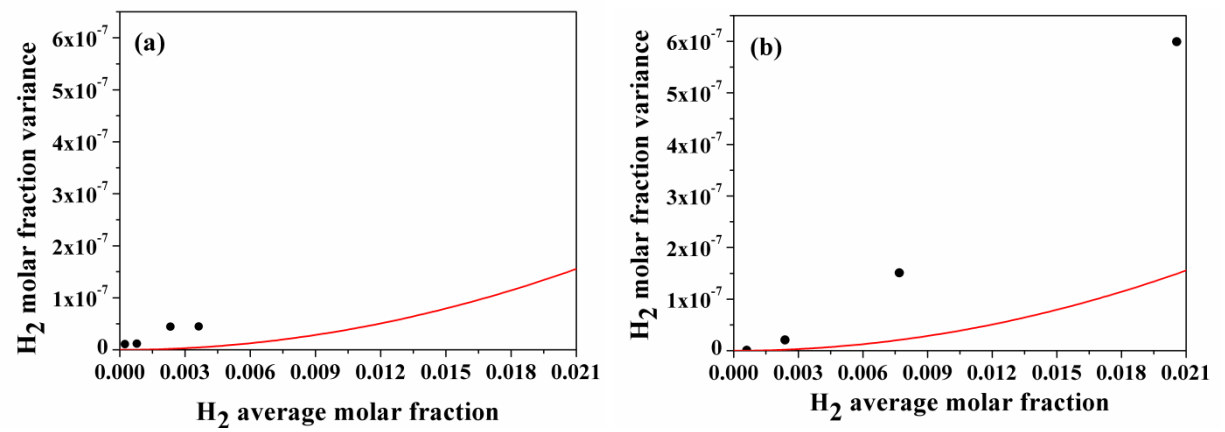

Figure 6 – Variances of hydrogen molar fractions for catalytic reactions (●) and chromatographic measurement fluctuation model (-) as functions of hydrogen average molar fractions for catalysts MgO-SiO_2-(50:50) (a) and MgO-SiO_2-(95:5) (b).

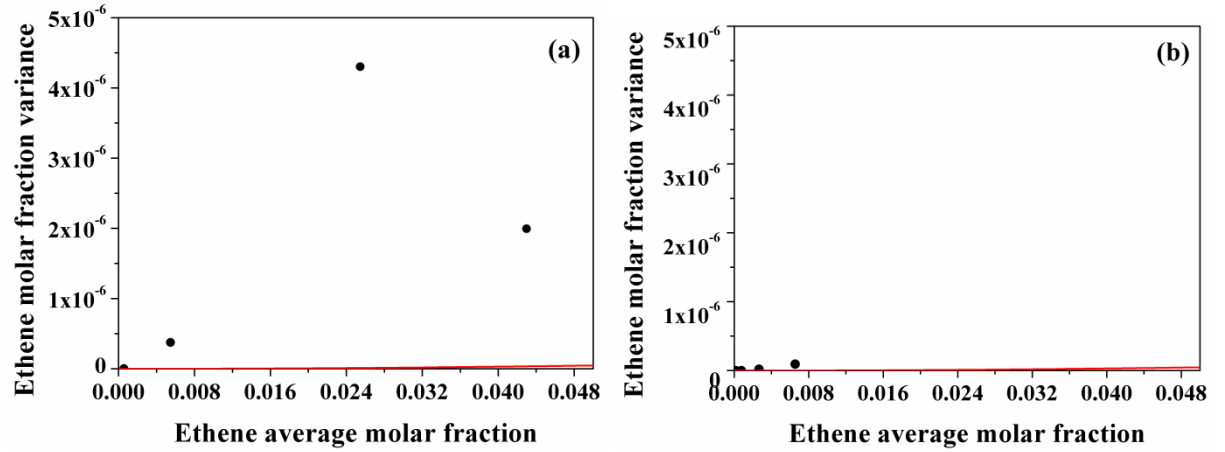

Figure 7 – Variances of ethene molar fractions for catalytic reactions (●) and chromatographic measurement fluctuation model (-) as functions of ethene average molar fractions for catalysts MgO-SiO_2-(50:50) (a) and MgO-SiO_2-(95:5) (b).

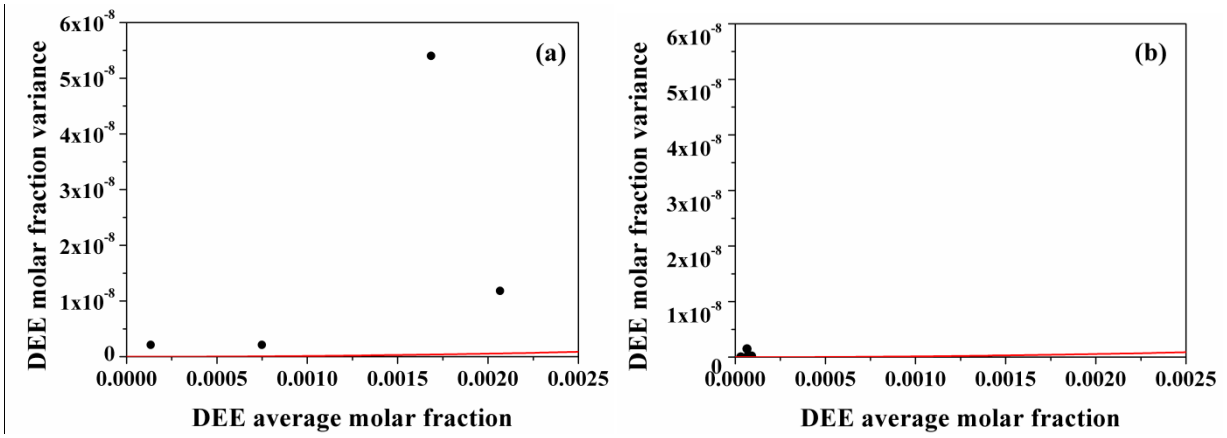

Figure 8 – Variances of DEE molar fractions for catalytic reactions (●) and chromatographic measurement fluctuation model (-) as functions of DEE average molar fractions for catalysts MgO-SiO_2-(50:50) (a) and MgO-SiO_2-(95:5) (b).

Whereas chromatographic measurement fluctuations increased with the respective average molar fraction, the same behavior was not observed for variances resulting from catalytic reactions. For instance, ethanol molar fractions variances in the output stream tended to decrease with the increase of the average molar fraction; that is, variances were reduced for low conversion values, as observed in reactions performed at 300 and 350 ºC, illustrated in Figure 3. Moreover, whilst variances obtained with the MgO-SiO_2-(50:50) catalyst were higher than variances observed for chromatographic analysis, variances obtained with the MgO-SiO_2-(95:5) catalyst were similar to them, as observed in Figures 3(b), 4(b) and 5(b). Therefore, reaction conditions, including catalyst properties, may result in completely different experimental fluctuation behavior. These results indicate once more that catalytic reaction fluctuations should not be regarded as constant throughout the analyzed experimental region during quantitative data analysis.

In order to emphasize the variance differences associated with the catalyst properties, Figure 9 shows variances of ethanol molar fraction measures obtained with catalysts MgO-SiO_2-(50:50) and MgO-SiO_2-(95:5). Dotted lines represent the upper and bottom 95% normal confidence limits for the assumption of similar variances, clearly

indicating that variances were consistently lower for catalyst MgO-SiO_2-(95:5) and that at least one pair of variances could not be regarded as similar for both catalysts. It should be noted that variances were obtained for ethanol molar fractions of similar orders of magnitude, as one can visualize in Tables 1 and 2. Thus, if catalyst properties did not exert any significant influence on variances of ethanol molar fractions, dots would be expected to be evenly distributed above and below the reference solid line in all cases, which could not be observed in the analyzed reaction runs. Therefore, it seems reasonable to assume that variances of ethanol molar fractions in the output stream depend on the analyzed catalyst.

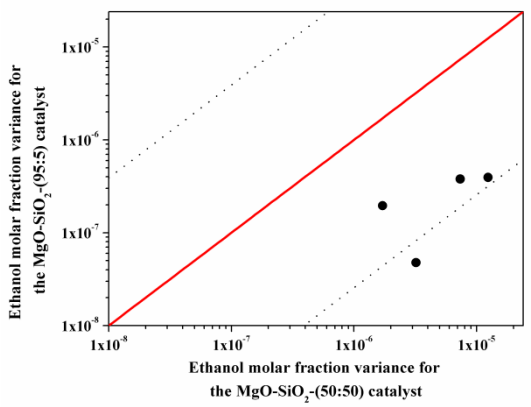

Figure 9 – Variances of ethanol molar fractions for catalysts MgO-SiO_2-(50:50) and MgO-SiO_2-(95:5).

Consequently, the larger catalytic reaction fluctuations observed in runs performed with catalyst MgO-SiO_2-(50:50) may contain significant amount of information about the reaction mechanism [19,30,31]. On the other hand, given the much lower fluctuation content in runs performed with catalyst MgO-SiO_2-(95:5), which were similar to the chromatographic measurement fluctuations, it may not be possible to obtain information about the reaction mechanism using the covariance matrix of catalytic reaction fluctuations for this catalytic system. Explaining why catalytic reaction fluctuations became much less important when the

Mg:Si molar ratio was changed from 50:50 to 95:5 is beyond the scope of the present work. However, a possible solution to allow the kinetic analysis of catalytic reaction fluctuations for the MgO-SiO_2-(95:5) system would be the determination of reaction conditions that would result in output compositions in the range where chromatographic measurement fluctuations attain the the smallest possible values.

3.4 *Principal Component Analysis*

It must be noted that the mechanistic interpretation based in the information contained in the covariance matrix of catalytic reaction fluctuations is only possible if it is assumed that the observed fluctuations of outlet stream compositions are governed by common sources of deviation, such as the intrinsic variability of catalyst activity. If fluctuations were governed by chromatographic measurement fluctuations, for instance, mechanistic interpretation of the covariance matrix would not make any sense, explaining why catalytic data obtained with the MgO-SiO_2-(95:5) catalyst cannot be used for kinetic interpretation.

In order to investigate whether fluctuations might have been induced by common sources of error, standard Principal Component Analysis (PCA) was performed with help of the software STATISTICA [34]. Significant PCA results (within the 95% confidence level) are presented in Table 3. According to the standard PCA procedure, the eigenvalues and eigenvectors of the covariance matrices of catalytic reaction fluctuations were computed at each particular experimental condition and ordered in series of decreasing magnitudes. Assuming that catalytic reaction fluctuations follow the normal probability distribution, the confidence regions of data fluctuations can be described by a hyper-ellipsoid in the measured variable space, whose axes may have different sizes and do not necessarily coincide with the coordinate axes of the analyzed measurement space [17]. In this case, the eigenvectors can be understood as the directions of variable fluctuation while the eigenvalues represent the relative importance of fluctuations along the distinct directions. Thus, if some of the

eigenvalues present much larger magnitudes than the remaining ones, this can possibly indicate that few sources of fluctuation perturb the measurements and that variable fluctuations respond simultaneously to few perturbations.

Table 3 Principal directions of fluctuation, computed with standard PCA tools.

	Temperature						
	300 ºC		350 ºC		400 ºC		450 ºC
	Factor 1	Factor 2	Factor 1	Factor 2	Factor 1	Factor 2	Factor 1
Ethene	**-0.926**	0.378	**-0.925**	-0.380	**-0.879**	0.475	**0.999**
1,3-BD	**-0.995**	0.096	**-0.912**	-0.411	**-0.954**	0.301	**0.936**
AcH	**-0.995**	0.099	**-0.995**	-0.093	**-0.929**	-0.368	**-0.999**
Ethanol	**0.969**	0.246	**0.939**	-0.345	**0.989**	-0.141	**-0.999**
DEE	**-0.980**	0.197	**-0.999**	-0.004	-0.141	**-0.989**	**-0.749**
H_2	-0.680	**-0.733**	-0.687	**0.726**	**-0.919**	-0.394	**0.988**
Explained Variance (%)	86.70	13.30	83.86	16.14	73.20	26.80	90.23

Numbers in bold are significant within the 95% confidence level.

PCA results are shown in Table 3 and support the hypothesis that few common sources of fluctuation perturb the experimental system, as only one direction concentrates the largest part of the experimental variance for all reaction temperatures (for instance, at 450 ºC, 90 % of the experimental variance was due to one fluctuation direction). This common source of catalytic reaction fluctuations can be associated with different variables that characterize the experimental setup [24]. For instance, the most important source of fluctuation is expected

to be the unavoidable variation of catalyst activity as a result of fluctuations of the reaction temperature, feed composition, catalyst mass or flow pattern in the catalyst bed.

Regardless of the true most important source of catalytic reaction fluctuations, the PCA shows that the covariance matrix of catalytic reaction fluctuations obtained through experimental replication can be valuable for interpretation of the ethanol to 1,3-BD reaction [19]. Moreover, PCA results highlight the relationship between the main reactant (ethanol) and the remaining products. From 300 to 400 °C, the vector coefficients of ethanol and of the other compounds have opposite signs, clearly indicating the roles of reactants and products. However, at 450 ºC these relationships vary, indicating that important mechanistic changes occur in the temperature range from 400 to 450 ºC, as it will be discussed in the next section.

3.5 Microkinetic Analysis of the Covariance Matrix of Catalytic Reaction Fluctuations

Molar fraction determined in the output stream obtained with catalyst MgO-SiO_2-(50:50), shown in Table 1, were used to compute the covariance matrix of composition measurements at each analyzed reaction condition using Eq. (2.2) and Eq. (2.3). Afterwards, the respective correlation matrix was calculated with Eq. (2.4). It could be clearly observed that molar fraction variances of the different compounds were not independent (correlation coefficients were significantly different from zero) and that the patterns of the observed correlations were different at distinct reaction temperatures, suggesting modification of the reaction mechanism with the increase of reaction temperature. Based on the calculated correlation coefficients, it seems clear that the common assumption of independent fluctuations (and diagonal covariance matrix of catalytic reaction fluctuations) should be avoided.

3.5.1 Correlations between Ethanol and Reaction Products

Figure 10 shows the correlation coefficients between ethanol and the remaining reaction products. It can be seen that correlation coefficients change smoothly and steadily as temperature increases, supporting the physical interpretation of obtained correlation values [19]. The correlation coefficient between ethanol and ethene showed negative values for all reaction temperatures, ranging from -0.7 to -1.0, indicating the strong negative correlation between ethanol and ethene molar fractions. Therefore, the amounts of ethanol and ethene fluctuate in opposite directions, as might already be expected, since ethene is a major product of ethanol dehydration, as described in Eq. (3.1).

$$C_2H_5OH \rightarrow C_2H_4 + H_2O \quad (3.1)$$

Negative correlation coefficients for all reaction temperatures were also observed between ethanol and hydrogen and ethanol and 1,3-BD for similar reasons. However, for AcH and DEE, ethanol correlation coefficients were negative at lower temperatures and strongly positive at 450 ºC, indicating a possible change in the mechanism of their production.

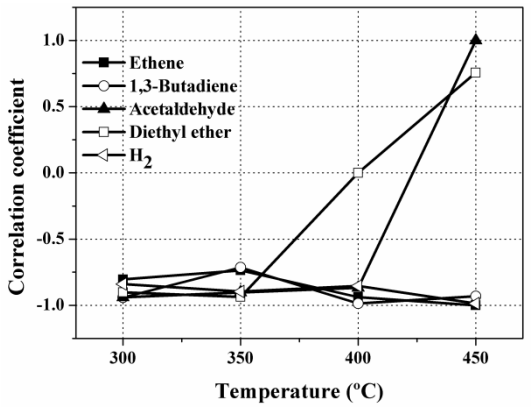

Figure 10 - Correlation coefficients between molar fractions of ethanol and of the major reaction products.

Ethanol dehydrogenation is favored thermodynamically as reaction temperature increases, being favorable in all reaction temperatures investigated in this study [15]. Thus, negative correlation coefficients between ethanol and AcH would be expected as ethanol is consumed in order to produce acetaldehyde, Eq. (3.2), as it was observed for correlation coefficients at temperatures ranging from 300 to 400 ºC.

$$C_2H_5OH \rightarrow CH_3CHO + H_2 \quad (3.2)$$

Nevertheless, AcH can also be produced in the proposed reaction mechanism in the crotyl alcohol formation step, where crotonaldehyde is reduced by ethanol, as illustrated in the reaction network of Figure 11.

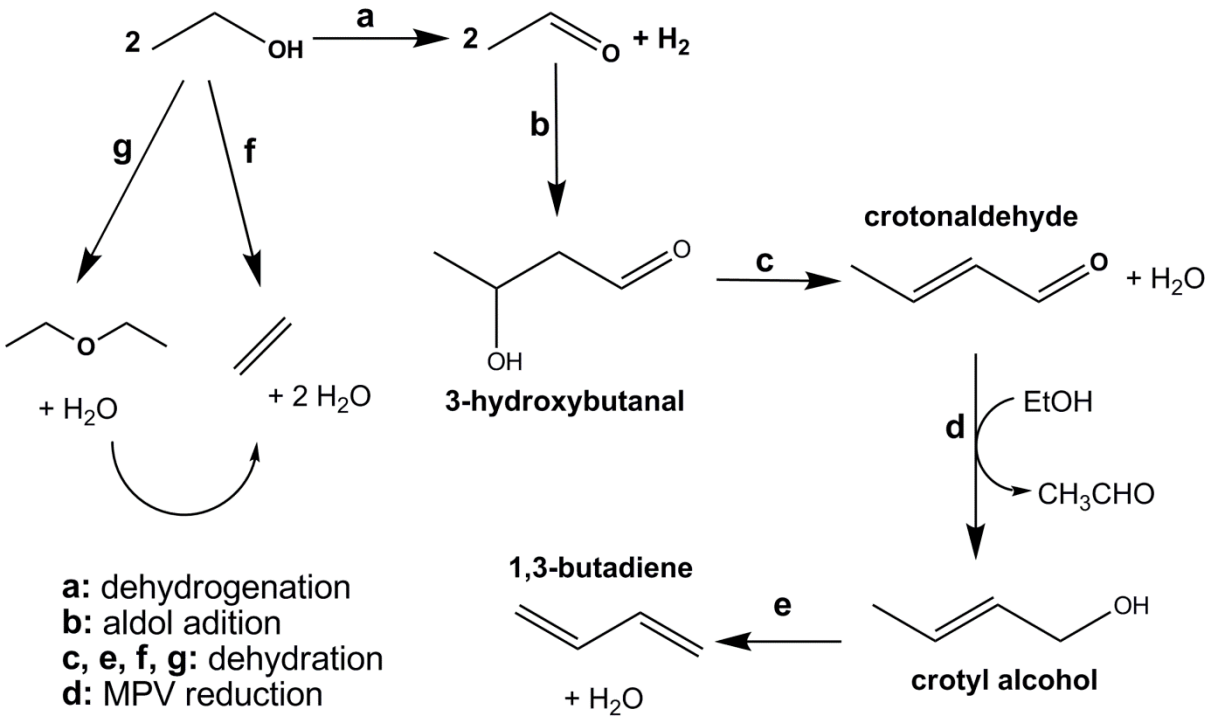

Figure 11 – Illustration of reaction network.

Whereas aldol addition is an endergonic reaction in the analyzed temperature range, becoming more endergonic as reaction temperature increases [15], 3-hydroxybutanal dehydration to crotonaldehyde is favorable in the analyzed temperature range, becoming more favorable as the reaction temperature increases. As discussed by Makshina *et al*. [15], AcH formation is favored thermodynamically at higher temperatures and the excess of AcH in the system can contribute to AcH condensation. Therefore, the positive correlation coefficient between AcH and ethanol at 450 ºC suggests that the rate of the rate determining step, which is probably related to the 3-hidroxybutanal formation from AcH, increases at this temperature, resulting in higher rates of AcH consumption. As a consequence, ethanol and AcH molar fractions tend to fluctuate in the same direction at such reaction condition.

In order to understand the behavior of the correlation coefficient between molar fractions of ethanol and DEE, it is convenient to analyze first the correlation coefficients between ethene and DEE.

3.5.2 Correlations involving Ethene and DEE

Figure 12 shows the correlation coefficients between ethene and the remaining compounds. It is possible to verify the strong linear relationship between the amounts of DEE and ethene, which was positive at 300 and 350 ºC and became negative as reaction temperature increased. It is well-known that DEE formation from ethanol, Eq. (3.3), is an exothermic reaction, while ethene formation from ethanol dehydration, Eq. (3.1), is an endothermic reaction [32]. Thus, the increase of reaction temperature favors the ethene formation and leads to decrease of DEE production. However, the strong negative relationship between ethene and DEE observed at 450 ºC can also be explained by DEE dehydration to ethene, Eq. (3.4) [7] and Figure 11. It must be noted that even under a kinetic regime, thermodynamic effects may contribute to changes on reaction rates, as equilibrium constants depend on temperature.

$$2C_2H_5OH \rightarrow (C_2H_5)_2O + H_2O \quad (3.3)$$

$$(C_2H_5)_2O \rightarrow 2C_2H_4 + H_2O \quad (3.4)$$

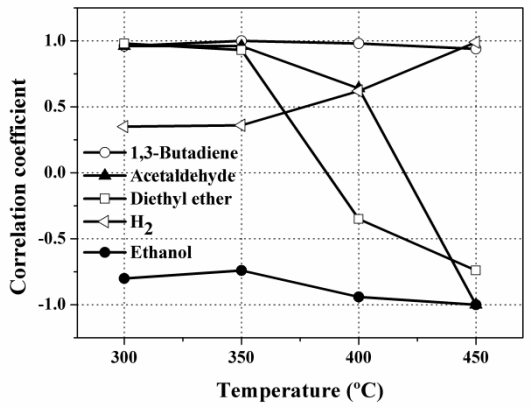

Figure 12 - Correlation coefficients between molar fractions of ethene and of the remaining major compounds.

Thus, at lower temperatures, both ethene and DEE are formed from ethanol. As reaction temperature increases, DEE can dehydrate to ethene and the production rate of DEE directly from ethanol decreases in respect to production rate of ethene. Both facts can explain why the amount of ethene and DEE change in opposite directions at 400 and 450 ºC. Therefore, the positive correlation coefficient observed between ethanol and DEE at 400 and 450 ºC can be understood as fluctuations that take place along the same direction because of the small oscillations of the reaction activity.

As illustrated in Figure 10, the correlation coefficient between ethanol and 1,3-BD showed negative values at all reaction temperatures, as expected because 1,3-BD is the most important final product of the consecutive reactions starting from ethanol. Moreover, 1,3-BD and ethene are both final products in two independent parallel reaction sequences from ethanol (see Figure 11), which can explain the positive correlation coefficients between ethene and 1,3-BD molar fractions at all reaction temperatures, as shown in Figure 12. The

positive correlation coefficients may also indicate that ethene and 1,3-BD do not compete for ethanol molecules, possibly suggesting the existence of excess of ethanol in the reacting system. Furthermore, the Prins reaction, which has been described as a possible route for 1,3-BD formation from ethene and AcH [33], according to Eq. (3.5), does not seem to occur in large extent due to the positive correlations between ethene and 1,3-BD, even though this reaction is thermodynamically possible at the analyzed temperature range [32]. As ethene and 1,3-BD are, respectively, reactant and product in Eq. (3.5), the significant occurrence of this reaction would probably lead to negative correlation coefficients between molar fractions of these two compounds (when 1,3-BD is produced, leading to higher 1,3-BD molar fractions, ethene is consumed, leading to lower ethene molar fractions). This finding is in accordance with the conclusions presented by Sushkevich *et al*. [7], who also ruled out the Prins reaction from experimental results obtained for different ethanol conversions.

$$C_2H_4 + CH_3CHO \rightarrow C_4H_6 + H_2O \quad (3.5)$$

Similarly to 1,3-BD, hydrogen is also a final product, in the sense that it is not consumed by other side reactions after formation at the analyzed reaction conditions. As a consequence, the correlation coefficient between ethene and hydrogen molar fractions presented the same trends of correlation coefficients between 1,3-BD and ethene molar fractions. On the other hand, correlation coefficients observed between AcH and ethene showed trends that were similar to the ones observed for correlation coefficients between ethene and DEE. This can be rationalized in terms of the rates of acetaldehyde consumption when the reaction temperature increases, while ethene molar fractions remain high.

Figure 13 shows the correlation coefficients between DEE and the other analyzed compounds. As DEE is formed at lower temperatures, correlation coefficients between DEE and the other products are also positive. At higher reaction temperatures, correlation

coefficient values become negative, indicating modification of the relative rates of some of the reactions that constitute this complex reaction system. The molar fraction of the final products, 1,3-BD, hydrogen and ethene, show negative correlation coefficients with DEE molar fraction at 450 ºC, probably because the latter is dehydrated to ethene. On the other hand, ethanol and AcH molar fractions show positive correlation coefficients with DEE, as ethanol, AcH and DEE are consumed at high rates at the highest reaction temperature.

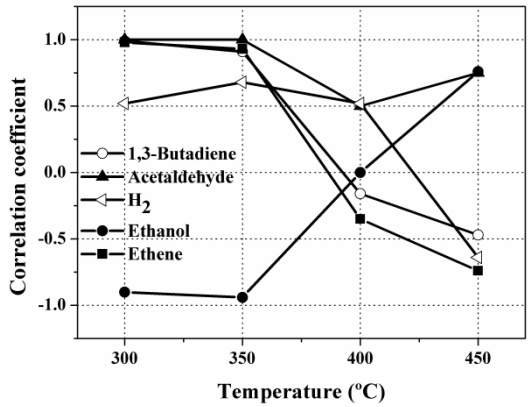

Figure 13 - Correlation coefficients between molar fractions of diethyl ether and of the remaining major compounds.

3.5.3 Correlations involving AcH and 1,3-BD

Correlation coefficients between molar fractions of AcH and of the other compounds are shown in Figure 14. Again, the positive correlation coefficients between AcH and ethanol, and AcH and DEE, highlight that AcH is consumed rapidly at 450 ºC. As 1,3-BD, hydrogen and ethene are produced at high rates at 450 ºC, correlation coefficients are negative in these cases. It is interesting to observe the relationship between 1,3-BD and AcH molar fractions, which clearly illustrate the modification of the relative rates of reaction. While from 300 to 400 ºC molar fractions of AcH and 1,3-BD were positively correlated, the correlation coefficient became negative at 450 ºC. This suggests that both 1,3-BD and AcH are formed in the system in the temperature range from 300 to 400 ºC, indicating that the acetaldehyde

condensation can be the slowest reaction step in this temperature range. However, at 450 ºC the rate of AcH consumption increases sharply, resulting in negative correlation coefficients between AcH and 1,3-BD molar fractions. Therefore, it can be suggested that the slowest reaction step at 450 ºC is related to the ethanol dehydrogenation.

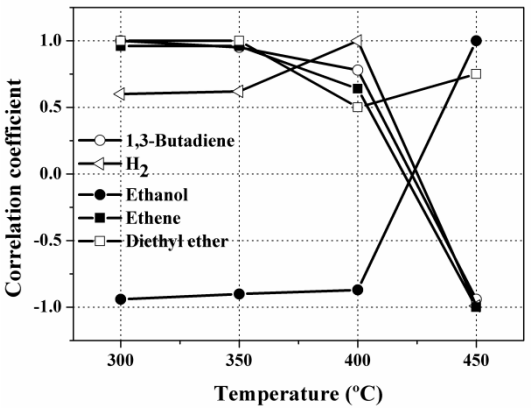

Figure 14. Correlation coefficients between molar fractions of acetaldehyde and of the remaining major compounds.

Finally, correlation coefficients between molar fractions of 1,3-BD and of other compounds are shown in Figure 15. The correlation coefficients between molar fractions of 1,3-BD and of other final products, such as hydrogen and ethene, are positive, indicating that these compounds are produced as reaction temperatures increase.

It has been discussed whether hydrogen could participate in the crotonaldehyde reduction, instead of ethanol [13]. As pointed out by some authors [13,32], hydrogen participation is less probable and, therefore, should not be involved in the crotyl alcohol formation. The positive correlation coefficients between 1,3-BD and hydrogen in Figure 15 support this hypothesis. If hydrogen was involved in the crotonaldehyde reduction, hydrogen would be consumed and a negative correlation coefficient between 1,3-BD and hydrogen molar fractions would be expected.

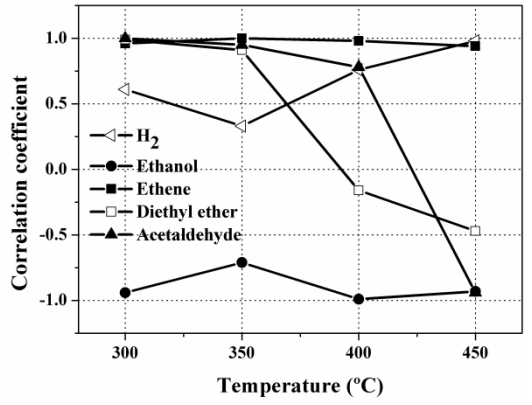

Figure 15 - Correlation coefficients between molar fractions of 1,3-butadiene and of the remaining major compounds.

The correlation analyses are in line with PCA results presented in the previous section, since the compounds that are also consumed at high rates at 450 ºC according to the previously discussed kinetic mechanism, that is, AcH and DEE, presented vector coefficients with the same sign of the vector coefficient of ethanol at this temperature, Table 3.

4. Conclusions

Experimental fluctuations (from chromatographic measurements and catalytic reactions) were characterized in ethanol to 1,3-butadiene reactions performed with MgO-SiO_2 catalysts. It was shown that both reaction temperature and catalyst properties affected the behavior of the catalytic reaction fluctuations significantly. Besides, it was shown that fluctuations of molar fraction of distinct compounds in the output stream were not independent and were statistically different at distinct reaction conditions, making the usual constant and independent error assumptions invalid for quantitative data analysis.

As the covariance matrices of catalytic reaction fluctuations could be discriminated from chromatographic measurement fluctuations, covariance matrices of catalytic reaction fluctuations were used for local microkinetic interpretation of the available data. Particularly, correlations analysis performed with data obtained with the MgO-SiO_2-(50:50) catalyst

indicated that the ethanol to 1,3-BD reaction mechanism probably involves two distinct slow steps in the analyzed temperature range. From 300 to 400 ºC, acetaldehyde condensation is expected to limit the reaction rates, while ethanol dehydrogenation is expected to be the slowest reaction step at 450 ºC. Standard PCA reinforced the proposed kinetic interpretation and indicated that variability of catalyst activity probably constitutes the most important source of experimental fluctuation in the analyzed reaction system.

5. Acknowledgment

The authors thank CNPq (Conselho Nacional de Desenvolvimento Científico e Tecnológico, Brazil) and FAPERJ (Fundação Carlos Chagas Filho de Apoio à Pesquisa do Estado do Rio de Janeiro) for supporting this research and providing scholarships.

Appendix A. Supporting Information

Supporting Information associated with this article can be found in the online version.

6. References

[1] J.A. Posada, A.D. Patel, A. Roes, K. Blok, A.P.C. Faaij, M.K. Patel, Potential of bioethanol as a chemical building block for biorefineries: preliminary sustainability assessment of 12 bioethanol-based products, Bioresour. Technol. 135 (2013) 490-499.

[2] G. Odian, Principles of polymerization, fourth ed., John Wiley & Sons, Inc., New York, 2004.

[3] H. Niiyama, S. Morii, E. Echigoya, Butadiene formation from ethanol over silica-magnesia catalysts, Bull. Chem. Soc. Jpn. 45 (1972) 655-659.

[4] S. Kvisle, A. Aguero, R.P.A. Sneeden, Transformation of ethanol into 1,3-butadiene over magnesium oxide/silica catalysts, Appl. Catal. 43 (1988) 117-131.

[5] M.D. Jones, C.G. Keir, C. Di Iulio, R.A.M. Robertson, C.V. Williams, D.C. Apperley, Investigations into the conversion of ethanol into 1,3-butadiene, Catal. Sci. Technol. 1 (2011) 267-272.

[6] E.V. Makshina, W. Janssens, B.F. Sels, P.A. Jacobs, Catalytic study of the conversion of ethanol into 1,3-butadiene, Catal. Today. 198 (2012) 338-344.

[7] V.L. Sushkevich, I.I. Ivanova, V.V. Ordomsky, E. Taarning, Design of a metal-promoted oxide catalyst for the selective synthesis of butadiene from ethanol, ChemSusChem. 7 (2014) 2527-36.

[8] M. Gao, Z. Liu, M. Zhang, L. Tong, Study on the mechanism of butadiene formation from ethanol, Catal. Lett. 144 (2014) 2071-2079.

[9] V.L. Sushkevich, I.I. Ivanova, E. Taarning, Ethanol conversion into butadiene over Zr-containing molecular sieves doped with silver, Green Chem. 17 (2015) 2552-59.

[10] S. Da Ros, M.D. Jones, D. Mattia, J.C. Pinto, M. Schwaab, F.B. Noronha, S.A. Kondrat, T.C. Clarke, S.H. Taylor, Ethanol to 1,3-butadiene conversion using ZrZn-containing MgO-SiO_2 systems prepared by co-precipitation and effect of catalyst acidity modification, ChemCatChem. 8 (2016) 2376-2386.

[11] W. Janssens, E.V. Makshina, P. Vanelderen, F. De Clippel, K. Houthoofd, S. Kerkhofs, J.A. Martens, P.A. Jacobs, B.F. Sels, Ternary Ag/MgO-SiO_2 catalysts for the conversion of ethanol into butadiene, ChemSusChem. 8 (2015) 994-1008.

[12] O.V. Larina, P.I. Kyriienko, S.O. Soloviev, Ethanol conversion to 1,3-butadiene on ZnO/MgO-SiO_2 catalysts: effect of ZnO content and MgO:SiO_2 ratio, Catal Letters. 145 (2015) 1162-1168.

[13] S.K. Bhattacharyya, S.K. Sanyal, Kinetic study on the mechanism of the catalytic conversion of ethanol to butadiene, J. Catal. 7 (1967) 152-158.

[14] C. Angelici, M.E.Z. Velthoen, B.M. Weckhuysen, P.C.A. Bruijnincx, Effect of preparation method and CuO promotion in the conversion of ethanol into 1,3-butadiene over SiO_2-MgO catalysts, ChemSusChem. 7 (2014) 2505-15.

[15] E.V. Makshina, M. Dusselier, W. Janssens, J. Degrève, P.A. Jacobs, B.F. Sels, Review of old chemistry and new catalytic advances in the on-purpose synthesis of butadiene, Chem. Soc. Rev. 43 (2014) 7917-53.

[16] G.F. Froment, K.B. Bischoff, J. De Wilde, Chemical reactor analysis and design, 3rd edition, John Wiley & Sons, Inc., 2011.

[17] M. Schwaab, E.C. Biscaia, Jr., J.L. Monteiro, J.C. Pinto, Nonlinear parameter estimation through particle swarm optimization, Chem. Eng. Sci. 63 (2008)1542-52.

[18] Y. Bard, Nonlinear Parameter Estimation, Pergamon Press, New York, 1974.

[19] A.L. Larentis, A.M.P. Bentes Jr., N.S. Resende, V.M.M. Salim, J.C. Pinto, Analysis of experimental errors in catalytic tests for production of synthesis gas, Appl. Catal. A. 242 (2003) 365-379.

[20] M. Schwaab, J.L. Monteiro, J.C. Pinto, Sequential experimental design for model discrimination taking into account the posterior covariance matrix of differences between model predictions, Chem. Eng. Sci. 63 (2008) 2408-19.

[21] H. Knözinger, K. Kochloefl, W. Meye, Kinetics of the bimolecular ether formation from alcohols over alumina, J. Catal. 28 (1973) 69-75.

[22] M. Schwaab, F.M. Silva, C.A. Queipo, A.G. Barreto Jr., M. Nele, J.C. Pinto, A new approach for sequential experimental design for model discrimination, Chem. Eng. Sci. 61 (2006) 5791-5806.

[23] A.L. Alberton, M. Schwaab, M.W.N. Lobão, J.C. Pinto, Experimental design for the joint model discrimination and precise parameter estimation through information measures, Chem. Eng. Sci. 66 (2011) 1940-52.

[24] A.L. Alberton, M. Schwaab, M. Schmal, J.C. Pinto, Experimental errors in kinetic tests and its influence on the precision of estimated parameters. Part I-Analysis of first-order reactions, Chem. Eng. J. 155 (2009) 816-823.

[25] M. Lewandowski, G.S. Babu, M. Vezzoli, M.D. Jones, R.E. Owen, D. Mattia, P. Plucinski, E. Mikolajska, A. Ochenduszko, D.C. Apperley. Investigations into the conversion of ethanol to 1,3-butadiene using MgO:SiO_2 supported catalysts, Catal. Commun. 49 (2014) 25-28.

[26] D.R.M. Brew, F.P. Glasser, Synthesis and characterisation of magnesium silicate hydrate gels, Cem. Concr. Res. 35 (2005) 85-98.

[27] J.S. Hartman, R.L. Millard, Gel synthesis of magnesium silicates: a ^{29}Si magic angle spinning NMR study, Phys. Chem. Minerals. 17 (1990) 1-8.

[28] D.C. Harris, Quantitative chemical analysis, seventh ed., W.H. Freeman and Company, New York, 2006.

[29] G.E.P. Box, W.G. Hunter, J.S. Hunter, Statistics for experimenters-An introduction to design, data analysis, and model building, John Wiley & Sons, New York, 1978.

[30] H.S. Cerqueira, R. Rawet, J.C. Pinto, The influence of experimental errors during laboratory evaluation of FCC catalysts, Appl. Catal. A. 181 (1999) 209-220.

[31] R. Rawet, H.S. Cerqueira, J.C. Pinto, The influence of covariances during laboratory evaluation of FCC catalysts, Appl. Catal. A. 207 (2001) 199-209.

[32] C. Angelici, B.M. Weckhuysen, P.C.A. Bruijnincx, Chemocatalytic conversion of ethanol into butadiene and other bulk chemicals, ChemSusChem. 6 (2013) 1595-614.

[33] V. Gruver, A. Sun, J.J. Fripiat, Catalytic properties of aluminated sepiolite in ethanol conversion, Catal. Lett. 34 (1995) 359-364.

[34] StatSoft Inc., 2325 East 13th Street, Tulsa, OK, USA, 1995.